Available online at www.sciencedirect.com
ScienceDirect
Journal of Computational Physics 227 (2008) 2387–2410
JOURNAL OF COMPUTATIONAL PHYSICS
www.elsevier.com/locate/jcp

A generalized discontinuous Galerkin (GDG) method for Schrödinger equations with nonsmooth solutions

Kai Fan, Wei Cai *, Xia Ji

Department of Mathematics and Statistics, University of North Carolina at Charlotte, Charlotte, NC 28223, United States

Received 21 February 2007; received in revised form 4 September 2007; accepted 22 October 2007
Available online 7 November 2007

Abstract

In this paper, we propose a new generalized discontinuous Galerkin (GDG) method for Schrödinger equations with nonsmooth solutions. The numerical method is based on a reformulation of Schrödinger equations, using split distributional variables and their related integration by parts formulae to account for solution jumps across material interfaces. The proposed GDG method can handle time dependent and nonlinear jump conditions $[\varphi] = f(\varphi^-, \varphi^+)$. Numerical results for 1D and 2D time dependent Schrödinger equations validate the high order accuracy and the flexibility of the method for various types of interface conditions.

AMS Subject classifications: 65N38; 78M25

Keywords: Discontinuous Galerkin method; Split distributions; Schrödinger equation

1. Introduction

In paraxial approximations for wave propagations [1,2] in optical waveguides, the time harmonic Maxwell's equations are approximated by Schrödinger equations where the propagation direction is identified as the time axis. Due to the mismatch of refractive indices in waveguides, the electromagnetic fields are discontinuous solutions to Schrödinger equations, a property not shared by the probability wave functions of quantum mechanics. In order to handle the discontinuities, we propose in this paper to reformulate the Schrödinger equations using distribution variables where Dirac δ-functions are introduced as source terms to account for the discontinuities in the solution and its derivatives. Discontinuous Galerkin projections of the distribution variables are then used to obtain numerical discretizations, thus the name ''generalized discontinuous Galerkin (GDG) method''.

The generalized discontinuous Galerkin (GDG) method extends the conventional discontinuous Galerkin methods to Schrödinger equations with general jump conditions at interfaces. Discontinuous Galerkin

* Corresponding author. Tel.: +1 704 687 4581; fax: +1 704 687 6415.
E-mail address: wcai@uncc.edu (W. Cai).

0021-9991/$ - see front matter © 2007 Elsevier Inc. All rights reserved.
doi:10.1016/j.jcp.2007.10.023

methods have been used to handle solutions with jumps, such as the shock waves for nonlinear hyperbolic systems. To account for those jumps, numerical fluxes are defined using local Riemann solvers for the hyperbolic systems [3–5]. Lately, the discontinuous Galerkin method has also been applied to elliptic problems [6–8] where the numerical fluxes enforce continuities of the solutions similar to the interior penalty methods proposed by Baker et al. [9–11]. In this paper the GDG method enforces the jump conditions at interfaces using Dirac δ-functions as source terms in the partial differential equations. Those δ-functions act as penalty terms in the "collocation" sense. Penalty terms using Lagrange multiplier have been used in the enforcement of boundary conditions [12] and the coupling of domain decomposition spectral element method [13]. The advantage of using the δ-functions are three folds: (1) It can handle jump relationships of a general form $[\varphi] = f(\varphi^-, \varphi^+), [\varphi] = \varphi^+ - \varphi^-$ where $f(\varphi^-, \varphi^+)$ can be nonlinear and time dependent functions. (2) The discontinuous Galerkin projection of the δ-functions is natural due to the weak form definition of the distribution variables. In fact, we will define Galerkin projection of an evenly split Dirac $\delta(x)$ function in the sense of $\int_{\pm a}^{0} v(x)\delta(x)\mathrm{d}x = \mp\frac{1}{2}v(0)$, for $a > 0$ and its related integration by parts formula. (3) The GDG approach can be easily extended to multi-dimensional problems and other types of PDEs of higher orders with non-smooth solutions.

The remaining part of the paper is organized as follows. In Section 2, we will give a model problem of optical wave propagation in layered media using paraxial approximations and the jump conditions for the resulting 1D Schrödinger equation. Section 3 will reformulate the 1D Schrödinger equation using distributional variables and also propose the generalized discontinuous Galerkin(GDG) method. Then, in Section 4, we extend the GDG method to 2D cases. Section 5 contains numerical results validating the high accuracy and convergence of the proposed GDG method and the flexibility of handling nonlinear time dependent jump conditions. Finally, Section 6 gives the conclusion of the paper.

2. Schrödinger equations with nonsmooth solutions: paraxial approximation of wave propagations

To motivate the work of the generalized discontinuous Galerkin (GDG) method, we present a model problem on the paraxial approximation of wave propagations in a 3-layer media with dissimilar dielectric constants.

Assuming no charge nor current source and time harmonic field (with frequency ω), we have the following time harmonic Maxwell equations

$$\begin{cases} \nabla \times \overrightarrow{E} &= -\mathrm{i}\omega\mu\overrightarrow{H}, \\ \nabla \times \overrightarrow{H} &= \mathrm{i}\omega\epsilon\overrightarrow{E}, \\ \nabla \cdot (\epsilon\overrightarrow{E}) &= 0, \\ \nabla \cdot (\mu\overrightarrow{H}) &= 0. \end{cases} \tag{1}$$

Combining the first two equations and solving for $\overrightarrow{E}$, we get the vector wave equation

$$\nabla \times \nabla \times \overrightarrow{E} = \omega^2\epsilon\mu\overrightarrow{E}, \tag{2}$$

which will lead to

$$\nabla^2\overrightarrow{E} + \omega^2\epsilon\mu\overrightarrow{E} = \nabla(\nabla \cdot \overrightarrow{E}). \tag{3}$$

Let us consider the case $\overrightarrow{E}$ is independent of y, namely

$$\overrightarrow{E} = \overrightarrow{E}(x, z), \tag{4}$$

and also ϵ is a piecewise constant, say

$$\epsilon = \begin{cases} \epsilon_1 & \text{in } \Omega_1 = \{a \leqslant x < \tau_1\}, \\ \epsilon_2 & \text{in } \Omega_2 = \{\tau_1 < x < \tau_2\}, \\ \epsilon_3 & \text{in } \Omega_3 = \{\tau_2 < x \leqslant\ b\}. \end{cases} \tag{5}$$

Then, we can decouple E_y from E_x and E_z in (3), and get the following scaler Helmholtz equation for E_y component

$$\nabla^2 E_y + \omega^2 \epsilon \mu E_y = 0, \quad \text{in } \Omega = [a,b] \setminus \{\tau_1, \tau_2\}, \tag{6}$$

with continuity at interface given as, for $k = 1, 2$,

$$E_y(\tau_k^-, z) = E_y(\tau_k^+, z), \tag{7}$$

$$\frac{\partial E_y(\tau_k^-, z)}{\partial x} = \frac{\partial E_y(\tau_k^+, z)}{\partial x}. \tag{8}$$

Now assume

$$E_y(x,z) = \varphi(x,z) e^{-i\beta_I z}, \quad \text{in } \Omega_I,\ I = 1,2,3, \tag{9}$$

where φ is an envelope function which varies slowly along the *propagation direction* z. By applying the slowly varying envelope approximation (paraxial approximation), i.e.

$$\left|\frac{\partial^2 \varphi}{\partial z^2}\right| \ll 2\beta_I \left|\frac{\partial \varphi}{\partial z}\right|, \tag{10}$$

we can ignore the second order derivative in z and get the following scalar beam propagation equation

$$i2\beta_I \frac{\partial \varphi}{\partial z} = \frac{\partial^2 \varphi}{\partial x^2} + (\omega^2 \epsilon_I \mu - \beta_I^2)\varphi, \quad \text{in } \Omega_I. \tag{11}$$

Choosing

$$\beta_I = \omega \sqrt{\epsilon_I \mu}, \tag{12}$$

we have

$$i2\beta_I \frac{\partial \varphi}{\partial z} = \frac{\partial^2 \varphi}{\partial x^2}, \quad \text{in } \Omega_I,\ I = 1,2,3, \tag{13}$$

with jump condition, for $k = 1, 2$,

$$e^{-i\beta_k z} \varphi(\tau_k^-, z) = e^{-i\beta_{k+1} z} \varphi(\tau_k^+, z), \tag{14}$$

$$e^{-i\beta_k z} \frac{\partial \varphi(\tau_k^-, z)}{\partial x} = e^{-i\beta_{k+1} z} \frac{\partial \varphi(\tau_k^+, z)}{\partial x}. \tag{15}$$

3. 1D GDG method

3.1. Distributional formulation of the Schrödinger equation with nonsmooth solutions

Replacing z by t in (13), we have the 1D Schrödinger equation with zero potential

$$ic \frac{\partial \varphi(x,t)}{\partial t} = \frac{\partial^2 \varphi(x,t)}{\partial x^2}, \quad \text{for } x \in [a,b] \setminus \{\tau_1, \tau_2\}, \tag{16}$$

where φ is a complex-valued wave function, and c is given as

$$c = 2\beta_I = 2\omega \sqrt{\epsilon_I \mu}, \quad \text{in } \Omega_I\ I = 1,2,3. \tag{17}$$

With the shorthand notation

$$[u(\tau_k, t)] = u(\tau_k^+, t) - u(\tau_k^-, t), \tag{18}$$

we can write the jump conditions at τ_k, $k = 1, 2$ as

$$[\varphi(\tau_k, t)] = f_k(t), \tag{19}$$

$$\left[\frac{\partial\varphi(\tau_k,t)}{\partial x}\right] = g_k(t), \tag{20}$$

which, from (14) and (15), are given by

$$f_k(t) = \frac{1}{2}\left(e^{i\frac{(c_{k+1}-c_k)}{2}t} - 1\right)\varphi(\tau_k^-,t) + \frac{1}{2}\left(1 - e^{i\frac{(c_k-c_{k+1})}{2}t}\right)\varphi(\tau_k^+,t), \tag{21}$$

$$g_k(t) = \frac{1}{2}\left(e^{i\frac{(c_{k+1}-c_k)}{2}t} - 1\right)\frac{\partial\varphi(\tau_k^-,t)}{\partial x} + \frac{1}{2}\left(1 - e^{i\frac{(c_k-c_{k+1})}{2}t}\right)\frac{\partial\varphi(\tau_k^+,t)}{\partial x}. \tag{22}$$

Next we incorporate the jump conditions into (16) using δ and δ' source terms at τ_1, τ_2, namely,

$$ic\frac{\partial\varphi(x,t)}{\partial t} = \frac{\partial^2\varphi(x,t)}{\partial x^2} - g_1(t)\delta(x-\tau_1) - g_2(t)\delta(x-\tau_2) - f_1(t)\delta'(x-\tau_1) - f_2(t)\delta'(x-\tau_2), \quad \text{for } x \in [a,b]. \tag{23}$$

The key idea here is the use of the δ and δ' source terms to compensate the singularity introduced by the jump conditions at interfaces. This approach of using δ functions to account for the jump conditions provides an alternative way to traditional interior penalty method [12,13], which uses Lagrange multipliers to enforce the continuities of solutions.

Remark 1. In the derivations above, we have selected different constant β_I for Ω_I in (12) for generality of jump conditions. In practice a single propagation constant β (obtained by solving the eigenmodes for the waveguide) is usually selected for the beam propagation method of wave propagation. For 3D problems, the electrical field will be discontinuous across interfaces of materials of dissimilar dielectric constants, the jumps in (21) and (22) will be nonzero in general.

3.2. 1D generalized discontinuous Galerkin (GDG) method

To avoid dealing with δ' in (23), we introduce an auxiliary distributional variable p to rewrite (23) as

$$ic\frac{\partial\varphi}{\partial t} = \frac{\partial p}{\partial x} - g_1(t)\delta(x-\tau_1) - g_2(t)\delta(x-\tau_2), \tag{24a}$$

$$p = \frac{\partial\varphi}{\partial x} - f_1(t)\delta(x-\tau_1) - f_2(t)\delta(x-\tau_2). \tag{24b}$$

Now, both φ, p are piecewise continuous functions over $[a,b]$, while $\frac{\partial\varphi}{\partial x}, \frac{\partial p}{\partial x}$ are treated as distributions.

To derive finite element approximation of (24a) and (24b), we first divide $\Omega = [a,b]$ into N segments as

$$\{a = x_0 < \cdots < x_{k_1} = \tau_1 < \cdots < x_{k_2} = \tau_2 < \cdots < x_N = b\}, \tag{25}$$

and denote element

$$K = [x_k, x_{k+1}], \quad \text{for } k = 0,\ldots,N-1. \tag{26}$$

To proceed, we will need the following evenly split δ-function

$$\int_{\pm a}^{0} v(x)\delta(x)\mathrm{d}x = \mp\frac{1}{2}v(0), \quad \text{for } a > 0,\ v(x) \in C(\pm a, 0], \tag{27}$$

and integration by parts identities for distributional variables $\frac{\partial\varphi}{\partial x}, \frac{\partial p}{\partial x}$ over closed interval,

$$\int_\tau^{\tau+h} \frac{\partial\varphi}{\partial x}v(x)\mathrm{d}x = \varphi(\tau+h)v(\tau+h) - \{\varphi\}v(\tau) - \int_\tau^{\tau+h}\frac{\partial v}{\partial x}\varphi(x)\mathrm{d}x, \tag{28}$$

$$\int_\tau^{\tau+h} \frac{\partial p}{\partial x}v(x)\mathrm{d}x = p(\tau+h)v(\tau+h) - \{p\}v(\tau) - \int_\tau^{\tau+h}\frac{\partial v}{\partial x}p(x)\mathrm{d}x, \tag{29}$$

where $\{u\} = \frac{1}{2}(u(\tau^+) + u(\tau^-))$ denotes the average of the values of function u at the interface $\tau = \tau_k$. The proofs of (27)–(29) are given in Appendix 1.

Let $P^J(K)$ be the space of polynomials in K of degree at most J, and $v \in L^1[a,b]$ be a test function, where $v|_K \in P^J(K)$ for $K = 0,\ldots,N-1$. Let us consider the first segment on the right of the interface, say $K = [x_{k_1}, x_{k_1+1}]$, $x_{k_1} = \tau_1$. By multiplying (24a) by v and integrating by part over K, we get

$$\begin{aligned} \mathrm{i}c\int_K \frac{\partial\varphi}{\partial t} v\,\mathrm{d}x &= pv|_{x_{k_1+1}^-} - \{p\}(\tau_1)v(x_{k_1}^+) - \int_K p\frac{\mathrm{d}v}{\mathrm{d}x}\,\mathrm{d}x - g_1(t)\int_K \delta(x-\tau_1)v\,\mathrm{d}x \\ &= pv|_{x_{k_1+1}^-} - (\{p\}(\tau_1) + \frac{1}{2}g_1(t))v(x_{k_1}^+) - \int_K p\frac{\mathrm{d}v}{\mathrm{d}x}\,\mathrm{d}x, \end{aligned} \tag{30}$$

where the factor $\frac{1}{2}$ in front of $g_1(t)$ comes from (27). Eq. (30) suggests that we should define the fluxes at the right hand side of the interface $x_{k_1}^+ = \tau_1^+$ as

$$h_\varphi(x_{k_1}^+) = \{p\}(x_{k_1}) + \frac{1}{2}g_1(t), \tag{31}$$

and at $x_{k_1+1}^-$ as

$$h_\varphi(x_{k_1+1}^-) = p(x_{k_1+1}^-). \tag{32}$$

Repeating the above for $K = [x_{k_1-1}, x_{k_1}]$, $x_{k_1} = \tau_1$, one gets the fluxes at the left hand side of the interface $x_{k_1}^- = \tau_1^-$ as

$$h_\varphi(x_{k_1}^-) = \{p\}(x_{k_1}) - \frac{1}{2}g_1(t), \tag{33}$$

and at $x_{k_1-1}^+$ as

$$h_\varphi(x_{k_1-1}^+) = p(x_{k_1-1}^+). \tag{34}$$

As the solution is continuous at $x_{k_1\pm1}$, we can replace (32) and (34) by

$$h_\varphi(x_{k_1\pm1}^\pm) = \{p\}(x_{k_1\pm1}). \tag{35}$$

Similarly, we can define the fluxes for p as

$$h_p(\tau_1^\pm) = \{\varphi\}(\tau_1) \pm \frac{1}{2}f_1(t), \tag{36}$$

$$h_p(x_{k_1\pm1}^\pm) = \{\varphi\}(x_{k_1\pm1}). \tag{37}$$

In general, for $K = [x_k, x_{k+1}]$, we will have the following Galerkin discretization for (24a) and (24b)

$$\mathrm{i}c\int_K \frac{\partial\varphi}{\partial t} v\,\mathrm{d}x = h_\varphi(x_{k+1}^-)v(x_{k+1}^-) - h_\varphi(x_k^+)v(x_k^+) - \int_K p\frac{\mathrm{d}v}{\mathrm{d}x}\,\mathrm{d}x, \tag{38}$$

$$\int_K pv\,\mathrm{d}x = h_p(x_{k+1}^-)v(x_{k+1}^-) - h_p(x_k^+)v(x_k^+) - \int_K \varphi\frac{\mathrm{d}v}{\mathrm{d}x}\,\mathrm{d}x, \tag{39}$$

where if $x_k \neq \tau_1, \tau_2$,

$$h_\varphi(x_k^\pm) = \{p\}(x_k), \tag{40}$$

$$h_p(x_k^\pm) = \{\varphi\}(x_k), \tag{41}$$

and at $\tau = \tau_k, k = 1, 2$

$$h_\varphi(\tau^\pm) = \{p\}(\tau) \pm \frac{1}{2}g_k(t), \tag{42}$$

$$h_p(\tau^\pm) = \{\varphi\}(\tau) \pm \frac{1}{2}f_k(t). \tag{43}$$

Remark 2. In (42) and (43), if we substitute $f_k(t) = [\varphi](\tau_k), g_k(t) = [\frac{\partial\varphi(\tau_k,t)}{\partial x}] = [p](\tau_k)$, the fluxes take a similar form of the LDG flux in [6,7] with $\frac{1}{2}$ weighting factor for the jumps of the solution. However, it should be noted that the generalized Galerkin approach provides the mathematical justification for the use of $\{\varphi\}, [\varphi]$ or

$\{p\}, [p]$ even when the solution and its derivatives are discontinuous at the interface. In Section 3.3, we will show the consistence of the numerical scheme using (42) and (43) at the material interface.

Remark 3. Away from the jump interface τ_k, other forms of numerical fluxes [6] including IP and LDG can be used in (40) and (41) to address the possible spurious modes of high order discontinuous Galerkin methods.

Let $\phi_j(x), j = 0, 1, \ldots, J$ be the basis functions, and we expand φ and p as

$$\varphi(x,t) = \sum_{j=0}^{J} \varphi_j(t)\phi_j(x), \quad p(x,t) = \sum_{j=0}^{J} p_j(t)\phi_j(x), \tag{44}$$

and in each K, by choosing the test function $v = \phi_l(x)$ for $l = 0, \ldots, J$, and denoting m_{lj} and m^x_{lj} as

$$m_{lj} = \int_K \phi_l \phi_j \, \mathrm{d}x, \quad m^x_{lj} = \int_K \frac{\mathrm{d}\phi_l}{\mathrm{d}x} \phi_j \, \mathrm{d}x, \tag{45}$$

we have

$$\mathrm{i}c \sum_j m_{lj} \frac{\mathrm{d}\varphi_j}{\mathrm{d}t} = h_\varphi(x_{k+1})\phi_l(x^-_{k+1}) - h_\varphi(x_k)\phi_l(x^+_k) - \sum_j m^x_{lj} p_j, \tag{46a}$$

$$\sum_j m_{lj} p_j = h_p(x_{k+1})\phi_l(x^-_{k+1}) - h_p(x_k)\phi_l(x^+_k) - \sum_j m^x_{lj} \varphi_j. \tag{46b}$$

Let us define the mass matrix M and the stiff matrix M^x

$$M = (m_{ij}), \quad M^x = (m^x_{ij}) \tag{47}$$

and the following vectors

$$\overrightarrow{\varphi} = [\varphi_0 \cdots \varphi_J]^{\mathrm{T}}, \quad \overrightarrow{p} = [p_0 \cdots p_J]^{\mathrm{T}}, \quad \overrightarrow{\phi} = [\phi_0 \cdots \phi_J]^{\mathrm{T}},$$

we get the following system of ODEs

$$\mathrm{i}c \frac{\mathrm{d}\overrightarrow{\varphi}}{\mathrm{d}t} = M^{-1}[h_\varphi(x_{k+1})\overrightarrow{\phi}(x^-_{k+1}) - h_\varphi(x^+_k)\overrightarrow{\phi}(x^+_k) - M^x\overrightarrow{p}], \tag{48a}$$

$$\overrightarrow{p} = M^{-1}[h_p(x^-_{k+1})\overrightarrow{\phi}(x^-_{k+1}) - h_p(x^+_k)\overrightarrow{\phi}(x^+_k) - M^x\overrightarrow{\varphi}], \tag{48b}$$

which can also be written for the primary variable $\overrightarrow{\varphi}$ after eliminating $\overrightarrow{p}$ as

$$\frac{\mathrm{d}\overrightarrow{\varphi}}{\mathrm{d}t} = S\overrightarrow{\varphi}. \tag{49}$$

Remark 4. (Stability of GDG) The stability of the GDG discretization of the Schrödinger Eq. (16) is related to the eigenvalue distribution of the derivative matrix S, which should have a strictly negative real part. This is confirmed by numerical calculations of the eigenvalues for matrix S with homogeneous end boundary conditions. Figs. 1 and 2 show the eigenvalues in the complex plane with negative real parts and very small imaginary parts for the cases of second order basis $J = 2$ and $N = 8, 32$, respectively. Further theoretical study of the stability of the GDG is needed.

3.3. Consistence of zeroth order 1D GDG method

In this subsection, we will demonstrate the consistence of the proposed GDG method (48a) and (48b) by deriving the truncation error of the 1D zeroth order case. The convergence of higher order GDG method will be verified with numerical tests in Section 5.

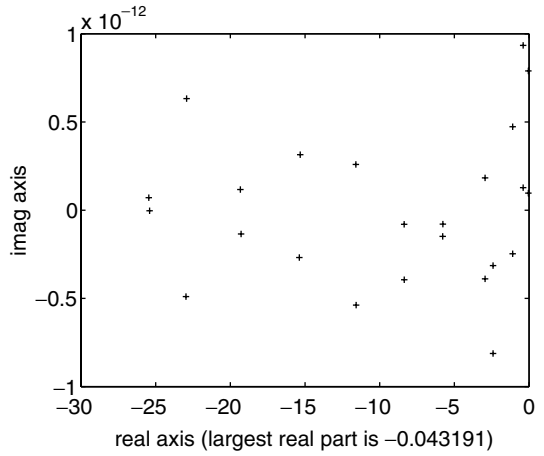

Fig. 1. Eigenvalues (scaled by $1/N^2$) of the matrix S in (49) for $J = 2$, $N = 8$.

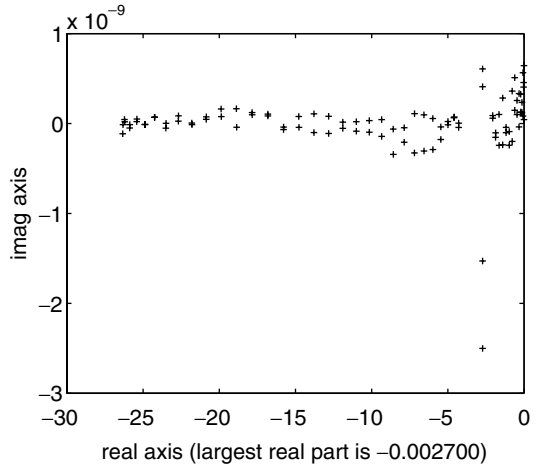

Fig. 2. Eigenvalues (scaled by $1/N^2$) of the matrix S in (49) for $J = 2$, $N = 32$.

First, we will find the equivalent finite difference formula by identifying the numerical solution as the approximation to the exact solution at the middle point $x_{i+\frac{1}{2}}$ of the interval $[x_i, x_{i+1}]$. And for simplicity, the location of the interface (jump) is set to be the origin. Let $\varphi(x, t)$ be the exact solution to the Schrödinger equation and the interface jump condition at $x = 0$ plus additional boundary conditions at the exterior boundaries (not shown in Fig. 3), then (24a) and (24b) becomes

$$\mathrm{i}c\frac{\partial \varphi}{\partial t} = \frac{\partial p}{\partial x} - g(t)\delta(x), \tag{50a}$$

$$p = \frac{\partial \varphi}{\partial x} - f(t)\delta(x), \tag{50b}$$

$$B_1[\varphi] \equiv \varphi(0^+, t) - \varphi(0^-, t) - f(t) = 0, \tag{50c}$$

$$B_2[\varphi] \equiv \frac{\partial \varphi(0^+, t)}{\partial x} - \frac{\partial \varphi(0^-, t)}{\partial x} - g(t) = 0. \tag{50d}$$

As shown in Fig. 3, over the four intervals around $x = 0$ we identify φ_{-1}, φ_0^-, φ_0^+, φ_1 as the approximations to $\varphi(-\frac{3h}{2})$, $\varphi(-\frac{h}{2})$, $\varphi(\frac{h}{2})$, $\varphi(\frac{3h}{2})$, respectively; p_{-1}, p_0^-, p_0^+, p_1 as the approximations to $\varphi'(-\frac{3h}{2})$, $\varphi'(-\frac{h}{2})$, $\varphi'(\frac{h}{2})$, $\varphi'(\frac{3h}{2})$, respectively.

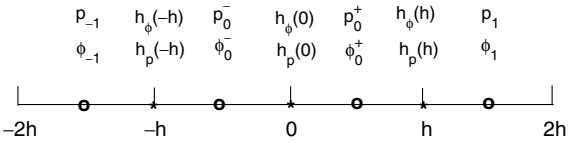

Fig. 3. 1D mesh near $x = 0$.

Meanwhile, h_φ and h_p are the numerical flux of φ and p, at $x = -h, 0^\pm, h$ given by (40)–(43), i.e.

$$h_\varphi(-h) = \frac{1}{2}p_{-1} + \frac{1}{2}p_0^-, \quad h_\varphi(0^\pm) = p_0^\pm, \quad h_\varphi(h) = \frac{1}{2}p_0^+ + \frac{1}{2}p_1, \tag{51}$$

$$h_p(-h) = \frac{1}{2}\varphi_{-1} + \frac{1}{2}\varphi_0^-, \quad h_p(0^\pm) = \varphi_0^\pm, \quad h_p(h) = \frac{1}{2}\varphi_0^+ + \frac{1}{2}\varphi_1. \tag{52}$$

The semi-discretized system (continuous in time) to (50a)–(50d) is given as

$$\begin{aligned}
&\mathrm{i}c\frac{\partial\varphi_0^\pm}{\partial t} = \mathcal{L}[\varphi_i, p_i]|_{0^\pm} \equiv \mp\frac{1}{h}(h_\varphi(0^\pm) - h_\varphi(\pm h)),\\
&p_0^\pm = \mp\frac{1}{h}(h_p(0^\pm) - h_p(\pm h)),\\
&\mathcal{B}_1[\varphi] \equiv (\varphi_0^+ - \varphi_0^-) - f(t) = 0,\\
&\mathcal{B}_2[\varphi] \equiv (p_0^+ - p_0^-) - g(t) = 0.
\end{aligned}$$

Using (51) and (52) to express p_0^-, p_0^+ in terms of φ as

$$p_0^\pm = \mp\frac{1}{h}(h_p(0^\pm) - h_p(\pm h)) = \mp\frac{1}{2h}(\varphi_0^\pm - \varphi_{\pm 1}),$$

we get

$$\mathrm{i}c\frac{\partial\varphi_0^-}{\partial t} = \frac{1}{4h^2}(\varphi_0^- - \varphi_{-1}) - \frac{1}{2h}p_{-1}, \tag{53}$$

$$\mathrm{i}c\frac{\partial\varphi_0^+}{\partial t} = \frac{1}{2h}p_1 - \frac{1}{4h^2}(\varphi_1 - \varphi_0^+). \tag{54}$$

Now, define the truncation errors for the interface conditions at $x = 0$ as

$$\begin{aligned}
T_{B_1}(\varphi) &\equiv \left(\varphi\left(\frac{h}{2}, t\right) - \varphi\left(-\frac{h}{2}, t\right)\right) - f(t),\\
T_{B_2}(\varphi) &\equiv \left(\frac{\partial\varphi}{\partial x}\left(\frac{h}{2}, t\right) - \frac{\partial\varphi}{\partial x}\left(-\frac{h}{2}, t\right)\right) - g(t),
\end{aligned}$$

and truncation errors at $x = 0^\pm$ for the semi-discretized finite difference scheme (53) and (54) as

$$\begin{aligned}
T_{0^-}[\varphi, p] &= \mathrm{i}c\frac{\partial\varphi}{\partial t} - \mathcal{L}[\varphi, p]|_{0^-} = \mathrm{i}c\frac{\partial\varphi}{\partial t} - \frac{1}{4h^2}\left(\varphi\left(-\frac{h}{2}, t\right) - \varphi\left(-\frac{3h}{2}, t\right)\right) + \frac{1}{2h}p\left(-\frac{3h}{2}, t\right),\\
T_{0^+}[\varphi, p] &= \mathrm{i}c\frac{\partial\varphi}{\partial t} - \mathcal{L}[\varphi, p]|_{0^+} = \mathrm{i}c\frac{\partial\varphi}{\partial t} - \frac{1}{2h}p\left(\frac{3h}{2}, t\right) + \frac{1}{4h^2}(\varphi\left(\frac{3h}{2}, t\right) - \varphi\left(\frac{h}{2}, t\right)).
\end{aligned}$$

By Taylor expansions at $x = 0^\pm, k = 1, 3,$

$$\varphi\left(\pm\frac{kh}{2}\right) = \varphi(0^\pm) \pm \frac{k}{2}h\varphi'(0^\pm) + \frac{k^2}{8}h^2\varphi''(0^\pm) + O(h^3), \tag{55}$$

$$p\left(\pm\frac{kh}{2}\right) = \varphi'(0^\pm) \pm \frac{k}{2}h\varphi''(0^\pm) + O(h^2), \tag{56}$$

and, using the Schrödinger equation $ic\frac{\partial\varphi}{\partial t} = \frac{\partial^2\varphi}{\partial x^2}$ at $x = 0^{\pm}$, one can get

$$T_{B_1}(\varphi) \equiv O(h), \quad T_{B_2}(\varphi) \equiv O(h), \quad T_{0^{\pm}}[\varphi, p] \equiv O(h).$$

4. 2D GDG method

In this section, we will extend the GDG method to 2D time dependent Schrödinger equations with non-smooth solutions. Let the solution domain Ω be decomposed into regions Ω_i with jumps across their interfaces, i.e. $\Omega = \cup_i \Omega_i$.

We consider the following time dependent scalar 2D Schrödinger equation, for $(x, y) \notin \Gamma = \cup_i \partial\Omega_i$

$$ic\frac{\partial\varphi}{\partial t} = \frac{\partial^2\varphi}{\partial x^2} + \frac{\partial^2\varphi}{\partial y^2} + S(\varphi), \tag{57}$$

where c is a constant in each Ω_i and S is a source term. The jumps at $(x^*, y^*) \in \Gamma$, are given as

$$f(x^*, y^*, t) = [\varphi(x^*, y^*, t)] = \varphi(x^{*^+}, y^{*^+}, t) - \varphi(x^{*^-}, y^{*^-}, t), \tag{58}$$

$$g(x^*, y^*, t) = \left[\frac{\partial\varphi(x^*, y^*, t)}{\partial n}\right] = \frac{\partial\varphi(x^{*^+}, y^{*^+}, t)}{\partial n} - \frac{\partial\varphi(x^{*^-}, y^{*^-}, t)}{\partial n} \tag{59}$$

where n is the normal of the interface Γ.

On the interface Γ, a local coordinate (ξ, η) will be introduced where ξ is along the normal direction and η is along the tangential direction(s). Following the same procedure as for (24a,24b), we can rewrite (57) as

$$ic\frac{\partial\varphi}{\partial t} = \frac{\partial p}{\partial x} + \frac{\partial q}{\partial y} - \delta(\xi - \xi^*)|\nabla\xi|^2 g + S, \tag{60a}$$

$$p = \frac{\partial\varphi}{\partial x} - \delta(\xi - \xi^*) f\frac{\partial\xi}{\partial x}, \tag{60b}$$

$$q = \frac{\partial\varphi}{\partial y} - \delta(\xi - \xi^*) f\frac{\partial\xi}{\partial y}. \tag{60c}$$

The justification for the δ-function terms are given in (A.25)–(A.27) of Appendix 2, which are used to compensate the singularities from the differentiations of the solutions across the interface Γ.

As in 1D case, to derive a Galerkin projection for (60a)–(60c), we will use the property of split distributions in the 2D case given in (A.15) and their integration by parts formula (A.16) and (A.17). Then, for each element K in the discretization of Ω, let $P^J(K)$ denote the space of polynomials in K of degree at most J, and $v \in L^1(\Omega)$ the test function, where $v|_K \in P^J(K)$. Multiplying Eqs. (60a)–(60c) by v and integrating by parts in K, we can get

$$ic\int_K \frac{\partial\varphi}{\partial t} = \int_{\partial K} h_\varphi^x v n_x \,ds - \int_K p\frac{\partial v}{\partial x}\,dx\,dy + \int_{\partial K} h_\varphi^y v n_y \,ds - \int_K q\frac{\partial v}{\partial y}\,dx\,dy + \int_K Sv\,dx\,dy, \tag{61a}$$

$$\int_K pv\,dx\,dy = \int_{\partial K} h_p v n_x \,ds - \int_K \varphi\frac{\partial v}{\partial x}\,dx\,dy, \tag{61b}$$

$$\int_K qv\,dx\,dy = \int_{\partial K} h_q v n_y \,ds - \int_K \varphi\frac{\partial v}{\partial y}\,dx\,dy, \tag{61c}$$

where (n_x, n_y) is the external normal of ∂K and $(h_\varphi^x, h_\varphi^y, h_p = h_q)$ are numerical fluxes, which relate to (p, q, φ) at ∂K, are given as, for $\vec{x} = (x, y) \in \partial K$,

$$h_\varphi^x(\vec{x}^{\pm}) = \{p\} \pm a^x, \quad h_\varphi^y(\vec{x}^{\pm}) = \{q\} \pm a^y, \quad h_p(\vec{x}^{\pm}) = \{\varphi\} \pm b, \tag{62}$$

where $+$ indicates the exterior side of the ∂K and a^x, a^y, b from jump conditions are defined as

$$(a^x, a^y, b) = \begin{cases} \left(\frac{1}{2}g|\nabla\xi|n_x, \frac{1}{2}g|\nabla\xi|n_y, \frac{1}{2}f\right), & \text{if } \Gamma \cap K \neq \emptyset \\ (0, 0, 0), & \text{if } \Gamma \cap K = \emptyset \end{cases}. \tag{63}$$

As in (40)–(43) for 1D case, simple averages are used in (62) for all element boundaries except the material interface, where averages plus/minus half of the jump are used.

Let $\phi_j(x,y)$, $j=0,1,\ldots,n_J$ be the basis functions, where n_J+1 is the number of basis functions required for Jth order approximation, and we expand φ, p, q as

$$\varphi=\sum_{j=0}^{n_J}\varphi_j(t)\phi_j(x,y),\quad q=\sum_{j=0}^{n_J}q_j(t)\phi_j(x,y),\quad p=\sum_{j=0}^{n_J}p_j(t)\phi_j(x,y), \tag{64}$$

and choose the test function $v(x,y)=\phi_l(x,y)$ for $l=0,1,\ldots,n_J$, we get

$$\mathrm{i}c\sum_j m_{lj}\frac{\mathrm{d}\varphi_j}{\mathrm{d}t}=\int_{\partial K}(h_\varphi^x n_x+h_\varphi^y n_y)\phi_l\,\mathrm{d}s-\sum_j(m_{lj}^x p_j+m_{lj}^y q_j)+s_l, \tag{65a}$$

$$\sum\nolimits_j m_{lj}p_j=\int_{\partial K}h_p n_x\phi_l\mathrm{d}s-\sum_j m_{lj}^x\varphi_j, \tag{65b}$$

$$\sum\nolimits_j m_{lj}q_j=\int_{\partial K}h_q n_y\phi_l\mathrm{d}s-\sum_j m_{lj}^y\varphi_j, \tag{65c}$$

where $s_l=\int_K S\phi_l\,\mathrm{d}x\,\mathrm{d}y$ and

$$m_{lj}=\int_K\phi_l\phi_j\,\mathrm{d}x\,\mathrm{d}y,\quad m_{lj}^x=\int_K\frac{\partial\phi_l}{\partial x}\phi_j\,\mathrm{d}x\,\mathrm{d}y,\quad m_{lj}^y=\int_K\frac{\partial\phi_l}{\partial y}\phi_j\,\mathrm{d}x\,\mathrm{d}y. \tag{66}$$

Now let us define the mass matrix M and the stiff matrices M^x, M^y as

$$M=(m_{ij}),\quad M^x=(m_{ij}^x),\quad M^y=(m_{ij}^y), \tag{67}$$

and the vectors

$$\overrightarrow{\varphi}=[\varphi_0,\ldots,\varphi_{n_J}]^{\mathrm{T}},\quad \overrightarrow{\phi}=[\phi_0,\ldots,\phi_{n_J}]^{\mathrm{T}},$$
$$\overrightarrow{p}=[p_0,\ldots,p_{n_J}]^{\mathrm{T}},\quad \overrightarrow{q}=[q_0,\ldots,q_{n_J}]^{\mathrm{T}},\quad \overrightarrow{s}=[s_0,\ldots,s_{n_J}]^{\mathrm{T}}.$$

In each K, we will get the following system of ODEs,

$$\mathrm{i}c\frac{\mathrm{d}\overrightarrow{\varphi}}{\mathrm{d}t}=M^{-1}\left(\int_{\partial K}(h_\varphi^x n_x+h_\varphi^y n_y)\overrightarrow{\phi}\,\mathrm{d}s-M^x\overrightarrow{p}-M^y\overrightarrow{q}+\overrightarrow{s}\right), \tag{68}$$

$$\overrightarrow{p}=M^{-1}\left(\int_{\partial K}h_p n_x\overrightarrow{\phi}\,\mathrm{d}s-M^x\overrightarrow{\varphi}\right), \tag{69}$$

$$\overrightarrow{q}=M^{-1}\left(\int_{\partial K}h_q n_y\overrightarrow{\phi}\,\mathrm{d}s-M^y\overrightarrow{\varphi}\right), \tag{70}$$

which will be solved by Runge–Kutta methods.

5. Numerical results

5.1. 1D numerical results

In the following numerical tests, the time derivatives in (48a) and (48b) are discretized with a fourth order Runge–Kutta method and the time step Δt is chosen based on an empirical formula $\Delta t\leqslant(\Delta x)^2/((2J+1)^2/*\ \lambda_{\max})$ where Δx is the element size and $\lambda_{\max}$ is the largest magnitude of the eigenvalues of matrix S in (49). All error plots and Tables are given at the final simulation time $t=8$.

5.1.1. Linear homogeneous jump conditions

We consider the 1D Schrödinger Eq. (16) with the following exact discontinuous solution

$$\varphi(x,t)=\begin{cases}\mathrm{e}^{\mathrm{i}E_1t}(A_1\mathrm{e}^{\mathrm{i}k_{x_1}x}+B_1\mathrm{e}^{-\mathrm{i}k_{x_1}x}), & x\in[-2,-1)\\ \mathrm{e}^{\mathrm{i}E_2t}(A_2\mathrm{e}^{\mathrm{i}k_{x_2}x}+B_2\mathrm{e}^{-\mathrm{i}k_{x_2}x}), & x\in(-1,1)\\ \mathrm{e}^{\mathrm{i}E_3t}(A_3\mathrm{e}^{\mathrm{i}k_{x_3}x}+B_3\mathrm{e}^{-\mathrm{i}k_{x_3}x}), & x\in(1,2]\end{cases}, \tag{71}$$

where $E_I=k_{x_I}^2/c_I$ for $I=1,2,3$.

In the numerical test, $\varphi(x, t = 7)$ is taken as the initial condition to yield a jump in the solution and exact boundary condition at $x = \pm 2$ are used. The parameters are chosen as $k_{x_1} = k_{x_2} = k_{x_3} = 4,\ c_1 = c_3 = 3,\ c_2 = 3.1, A_1 = A_3 = e^{i(E_2 - \frac{c_2}{2})t}, A_2 = e^{i(E_1 - \frac{c_1}{2})t},\ B_1 = B_2 = B_3 = 0$. In this case the jump conditions are given by (21) and (22) with $\epsilon_1 = \epsilon_3 = 1.5^2$, $\epsilon_2 = 1.55^2$ and $\omega = 1$ for the c_k in (17).

Figs. 4 and 5 are plots of the numerical solutions vs exact solutions at $t = 8$. Fig. 6 is the convergence plot for $J = 0, 1, 2, 3$ with $N = 32$. Fig. 7 is the log error plot for $N = 8, 16, 32$ with $J = 2$. Meanwhile, Table 1 is the L^2 errors for $N = 8, 16, 32$ with $J = 1, 2, 3$.

5.1.2. Linear inhomogeneous jump conditions

As an example of inhomogeneous interface condition, we add an inhomogeneous term in each of (14) and (15), for $k = 1, 2$,

$$e^{-i\beta_k t}\varphi(\tau_k^-, t) = e^{-i\beta_{k+1} t}\varphi(\tau_k^+, t) + q_{2k-1}, \tag{72}$$

$$e^{-i\beta_k t}\frac{\partial\varphi(\tau_k^-, t)}{\partial x} = e^{-i\beta_{k+1} t}\frac{\partial\varphi(\tau_k^+, t)}{\partial x} + q_{2k}. \tag{73}$$

then, (21) and (22) should be modified as

$$f_k(t) = \frac{1}{2}\left[\left(e^{i\frac{(c_{k+1}-c_k)}{2}t} - 1\right)\varphi(\tau_k^-, t) + \left(1 - e^{i\frac{(c_k - c_{k+1})}{2}t}\right)\varphi(\tau_k^+, t) - q_{2k-1}\left(e^{i\frac{c_k}{2}t} + e^{i\frac{c_{k+1}}{2}t}\right)\right], \tag{74}$$

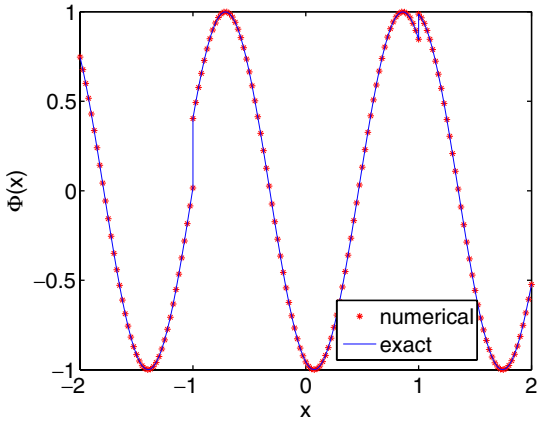

Fig. 4. Real part for the case of linear homogeneous jump.

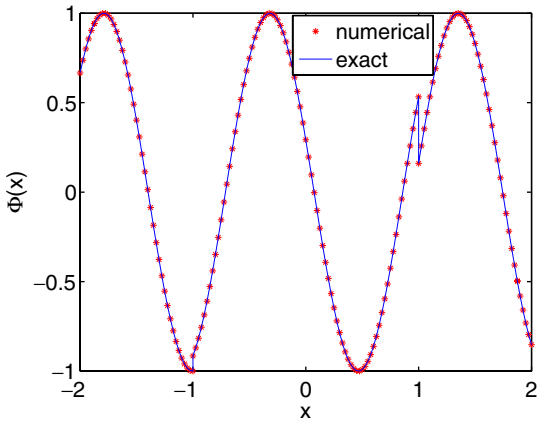

Fig. 5. Imaginary part for the case of linear homogeneous jump.

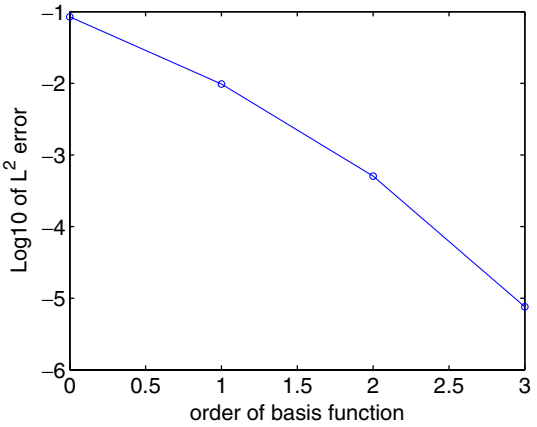

Fig. 6. Exponential decay of the L^2 error with increasing order of basis for the case of 1D linear homogeneous jump.

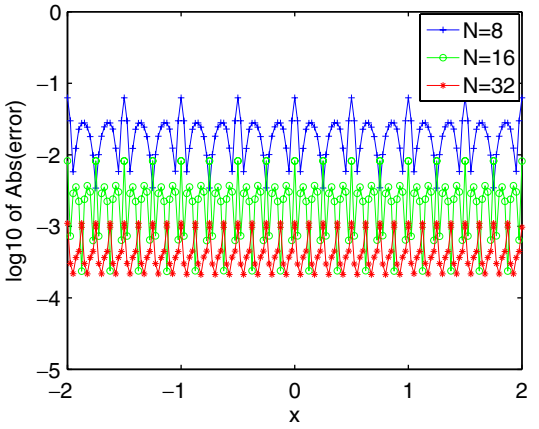

Fig. 7. The log error with decreasing mesh size for second order basis $J = 2$ for the case of 1D linear homogeneous jump.

Table 1
L^2 errors with $J = 1$, 2, 3 for the case of 1D linear homogeneous jump

	$J=1$			$J=2$			$J=3$		
N	Δt	L^2	Order	Δt	L^2	Order	Δt	L^2	Order
8	4e−3	9.0711e−2	–	4e−4	3.3388e−2	–	4e−5	1.2149e−3	–
16	1e−3	4.2692e−2	1.0872	1e−4	4.3116e−3	2.9530	1e−5	1.0722e−4	3.5022
32	2.5e−4	9.8135e−3	2.1211	2.5e−5	5.0634e−4	3.0900	2.5e−6	7.5933e−6	3.8197

$$g_k(t) = \frac{1}{2}\left[\left(e^{i\frac{(c_{k+1}-c_k)}{2}t} - 1\right)\frac{\partial\varphi(\tau_k^-,t)}{\partial x} + \left(1 - e^{i\frac{(c_k-c_{k+1})}{2}t}\right)\frac{\partial\varphi(\tau_k^-,t)}{\partial x} - q_{2k}\left(e^{i\frac{c_k}{2}t} + e^{i\frac{c_{k+1}}{2}t}\right)\right]. \tag{75}$$

For this case, the exact solution is

$$\varphi(x,t) = \begin{cases} e^{iE_1 t}\left(A_1 e^{ik_{x_1}x} + B_1 e^{-ik_{x_1}x}\right) + \widehat{A}_1 x + \widehat{B}_1, & x \in [-2,-1) \\ e^{iE_2 t}\left(A_2 e^{ik_{x_2}x} + B_2 e^{-ik_{x_2}x}\right) + \widehat{A}_2 x + \widehat{B}_2, & x \in (-1,1) \\ e^{iE_3 t}\left(A_3 e^{ik_{x_3}x} + B_3 e^{-ik_{x_3}x}\right) + \widehat{A}_3 x + \widehat{B}_3, & x \in (1,2] \end{cases} \tag{76}$$

where the parameters are chosen as $k_{x_1} = k_{x_2} = k_{x_3} = 4, c_1 = c_3 = 3, c_2 = 3.1, A_1 = A_3 = e^{i(E_2 - \frac{c_2}{2})t}, A_2 = e^{i(E_1 - \frac{c_1}{2})t}$, $B_1 = B_2 = B_3 = 0, \widehat{A}_1 = \widehat{A}_3 = e^{-i\frac{c_2}{2}t}, \widehat{A}_2 = e^{-i\frac{c_1}{2}t} + 0.2e^{i\frac{c_2}{2}t}, \widehat{B}_1 = \widehat{B}_3 = e^{-i\frac{c_2}{2}t}, \widehat{B}_2 = e^{-i\frac{c_1}{2}t} + 0.1e^{i\frac{c_2}{2}t}$, so that the jump

conditions are given by (74) and (75) for $\epsilon_1 = \epsilon_3 = 1.5^2$, $\epsilon_2 = 1.55^2$ and $\omega = 1$ for the c_k in (17) and $q_1 = 0.1$, $q_2 = -0.2$, $q_3 = -0.1$, $q_4 = 0.2$. $\varphi(t = 7)$ is chosen as the initial condition.

Figs. 8 and 9 are plots of the numerical solutions vs exact solutions at $t = 8$. Fig. 10 is the convergence plot for $J = 0, 1, 2, 3$ with $N = 32$. Fig. 11 is the log error plot for $N = 8, 16, 32$ with $J = 2$. And Table 2 is the L^2 errors for $N = 8, 16, 32$ with $J = 1, 2, 3$.

5.1.3. Nonlinear jump conditions

Next, we consider nonlinear jump conditions, we choose the parameters in (76) as $k_{x_1} = 2$, $k_{x_2} = 4$, $k_{x_3} = -2$, $c_1 = c_3 = 3$, $c_2 = 3.1$, $A_1 = e^{\frac{1}{2}i(E_2 t - k_{x_2})}$, $A_2 = e^{2i(E_1 t - k_{x_1})}$, $A_3 = e^{\frac{1}{2}i(E_2 t - k_{x_2})}$, $B_1 = B_2 = B_3 = 0$, $\widehat{A}_1 = \widehat{A}_2 = \widehat{A}_3 = 0$, $\widehat{B}_1 = \widehat{B}_2 = \widehat{B}_3 = 0$, so that we will have the following nonlinear jump conditions

$$\varphi^2(-1^-) = \varphi(-1^+), \quad \left(\frac{\partial\varphi(-1^-)}{\partial x}\right)^2 = i\frac{\partial\varphi(-1^+)}{\partial x}, \quad \varphi(1^-) = \varphi^2(1^+), \quad i\frac{\partial\varphi(1^-)}{\partial x} = \left(\frac{\partial\varphi(1^+)}{\partial x}\right)^2,$$

and, correspondingly, we have in (21) and (22)

$$f_1(t) = \frac{1}{2}(\varphi^2(-1^-) - \varphi(-1^-)) + \frac{1}{2}(\varphi(-1^+) - \varphi^{\frac{1}{2}}(-1^+)),$$
$$f_2(t) = \frac{1}{2}(\varphi^{\frac{1}{2}}(1^-) - \varphi(1^-)) + \frac{1}{2}(\varphi(1^+) - \varphi^2(1^+)),$$

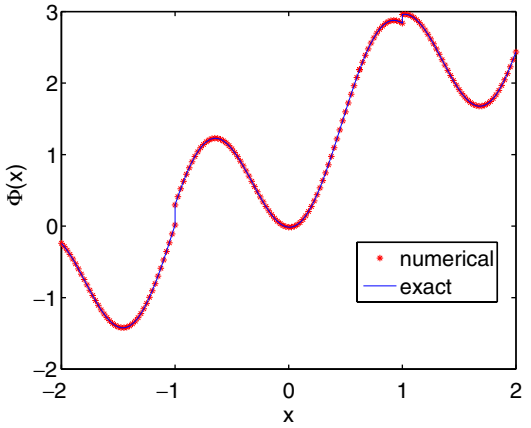

Fig. 8. Real part for the case of linear inhomogeneous jump.

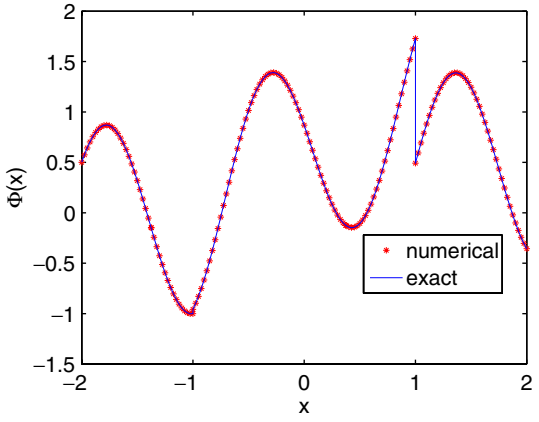

Fig. 9. Imaginary part for the case of linear inhomogeneous jump.

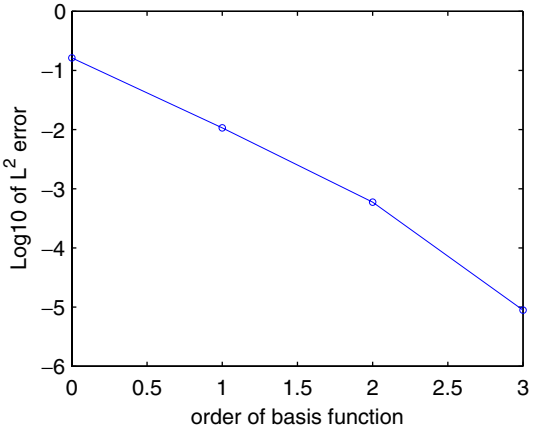

Fig. 10. Exponential decay of the L^2 error with increasing order of basis for the case of 1D inhomogeneous jump.

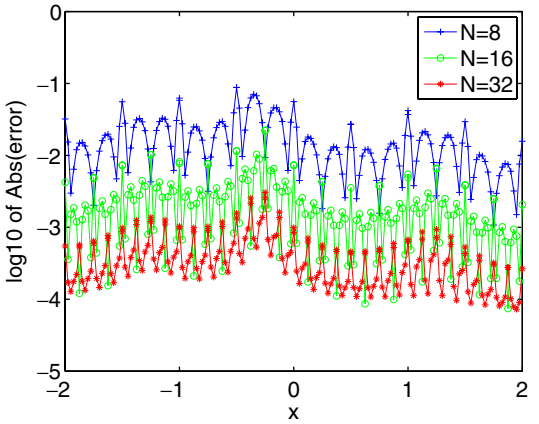

Fig. 11. The log error with decreasing mesh size for second order basis $J = 2$ for the case of 1D inhomogeneous jump.

Table 2
L^2 errors with $J = 1, 2, 3$ for the case of 1D linear inhomogeneous jump

	$J=1$			$J=2$			$J=3$		
N	Δt	L^2	Order	Δt	L^2	Order	Δt	L^2	Order
8	4e−3	1.8203e−1	–	4e−4	3.6616e−2	–	4e−5	1.4220e−3	–
16	1e−3	4.9122e−2	1.8897	1e−4	5.0381e−3	2.8615	1e−5	1.2580e−4	3.4987
32	2.5e−4	1.0682e−3	2.2011	2.5e−5	5.9317e−4	3.0863	2.5e−6	8.8845e−6	3.8236

$$g_1(t) = \frac{1}{2}\left(-\mathrm{i}\left(\frac{\partial\varphi(-1^-)}{\partial x}\right)^2 - \frac{\partial\varphi(-1^-)}{\partial x}\right) + \frac{1}{2}\left(\frac{\partial\varphi(-1^+)}{\partial x} - \left(\mathrm{i}\frac{\partial\varphi(-1^+)}{\partial x}\right)^{\frac{1}{2}}\right),$$

$$g_2(t) = \frac{1}{2}\left(\left(\mathrm{i}\frac{\partial\varphi(1^-)}{\partial x}\right)^{\frac{1}{2}} - \frac{\partial\varphi(1^-)}{\partial x}\right) + \frac{1}{2}\left(\frac{\partial\varphi(1^+)}{\partial x} + \mathrm{i}\left(\frac{\partial\varphi(1^+)}{\partial x}\right)^2\right).$$

$\varphi(t = 7)$ is chosen as the initial condition. Figs. 12 and 13 are plots of the numerical solutions vs exact solutions at $t = 8$. Fig. 14 is the convergence plot for $J = 0, 1, 2, 3$ with $N = 32$. Fig. 15 is the log error plot for $N = 8, 16, 32$ with $J = 2$. And Table 3 is the L^2 errors for $N = 8, 16, 32$ with $J = 1, 2, 3$.

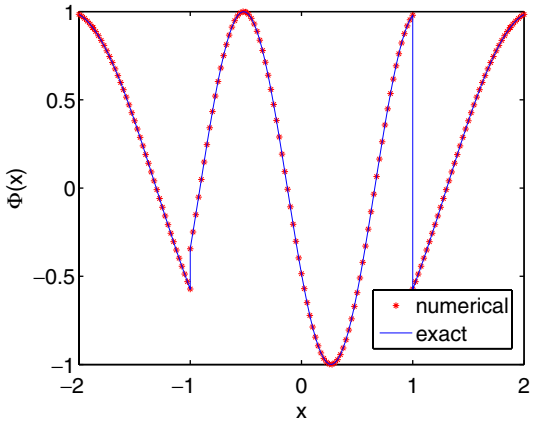

Fig. 12. Real part for the case of nonlinear jump.

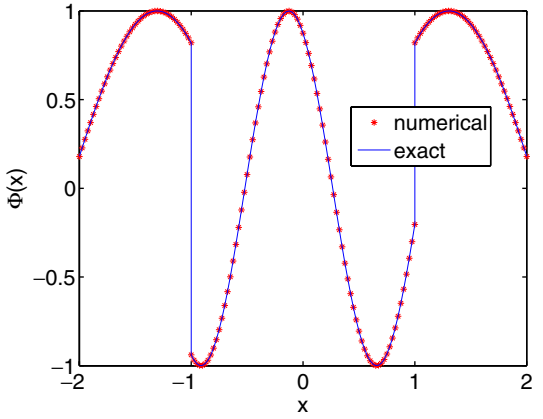

Fig. 13. Imaginary part for the case of nonlinear jump.

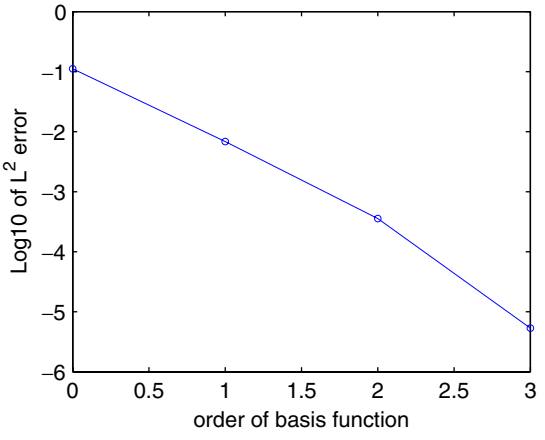

Fig. 14. Exponential decay of the L^2 error with increasing order of basis for the case of 1D nonlinear jump.

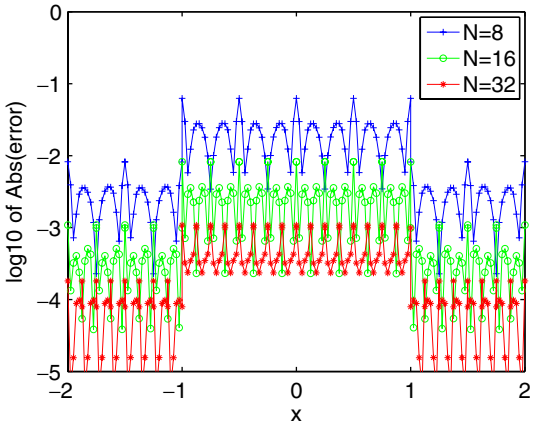

Fig. 15. The log error with decreasing mesh size for second order basis $J = 2$ for the case of 1D nonlinear jump.

Table 3
L^2 errors with $J = 1, 2, 3$ for the case of 1D nonlinear jump

	$J = 1$			$J = 2$			$J = 3$		
N	Δt	L^2	Order	Δt	L^2	Order	Δt	L^2	Order
8	4e−3	1.6756e−1	–	4e−4	2.3174e−2	–	4e−5	8.6352e−4	–
16	1e−3	3.5579e−2	2.2356	1e−4	3.0480e−3	2.9266	1e−5	7.5649e−5	3.5128
32	2.5e−4	6.8577e−3	2.3752	2.5e−5	3.5683e−4	3.0945	2.5e−6	5.3475e−6	3.8223

5.2. 2D numerical result

Assuming that the time dependent factor is e^{iEt}, the exact solution to a 2D scalar Schrödinger equation

$$ic\frac{\partial\varphi}{\partial t} = \nabla^2\varphi(x, y, t)$$

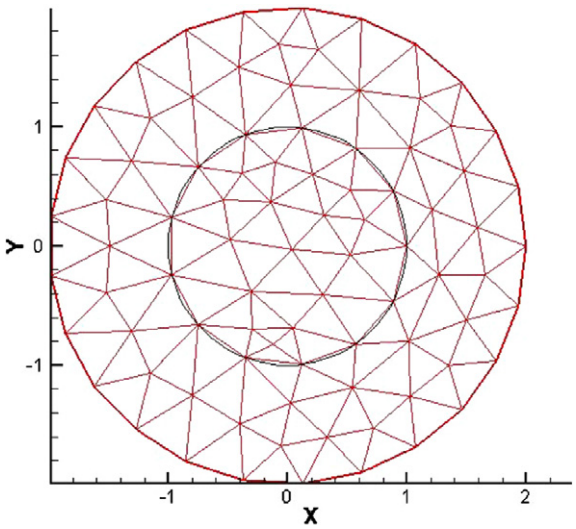

Fig. 16. 2D mesh.

given as

$$\varphi(x,t) = \begin{cases} e^{iE_1 t}(A_1 e^{ik_{x_1}x+ik_{y_1}y} + B_1 e^{-ik_{x_1}x-ik_{y_1}y}), & x \in \Omega_1 \\ e^{iE_2 t}(A_2 e^{ik_{x_2}x+ik_{y_2}y} + B_2 e^{-ik_{x_2}x-ik_{y_2}y}), & x \in \Omega_2 \end{cases} \tag{77}$$

where $E_i = (k_{x_i}^2 + k_{y_i}^2)/c_i$ for $i = 1, 2$, and

$$\Omega_1 = \{(x,y)|x^2 + y^2 \leqslant 1\}, \quad \Omega_2 = \{(x,y)|1 \leqslant x^2 + y^2 \leqslant 2\}. \tag{78}$$

The parameters are chosen as $k_{x_1} = k_{x_2} = k_{y_1} = 2$, $k_{y_2} = 3$, $c_1 = 3$, $c_2 = 3.1$, $A_1 = A_2 = 1$, $B_1 = B_2 = 0$ and jump given at interface $(x^2 + y^2 = 1)$ are

$$f(x,y,t) = e^{iE_2 t} e^{ik_{x_2}x+ik_{y_2}y} - e^{iE_1 t} e^{ik_{x_1}x+ik_{y_1}y},$$
$$g(x,y,t) = e^{iE_2 t}(ik_{x_2}x + ik_{y_2}y)e^{ik_{x_2}x+ik_{y_2}y} - e^{iE_1 t}(ik_{x_1}x + ik_{y_1}y)e^{ik_{x_1}x+ik_{y_1}y}.$$

Fig. 16 is the mesh used in the computation. Starting from $t = 0$, solution is computed up to $t = 1$ with a time step $\Delta t = 1e - 6$. Figs. 17 and 18 are real and imaginary part of the numerical results using a 3-rd order basis, respectively while Fig. 19 is the error plot. The exponential convergence is shown in Fig. 20.

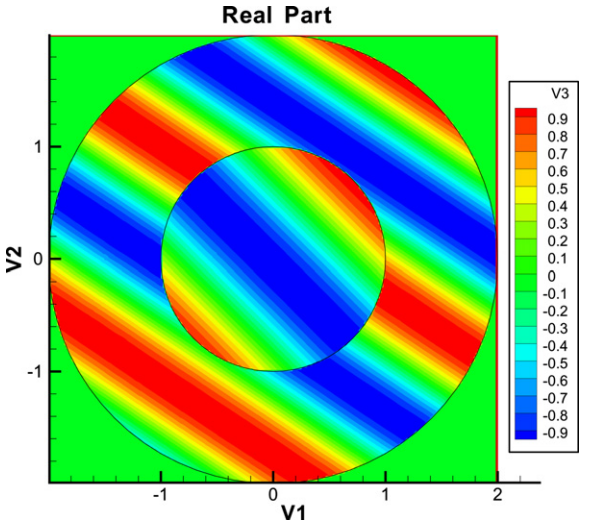

Fig. 17. Real part with third order basis for 2D case.

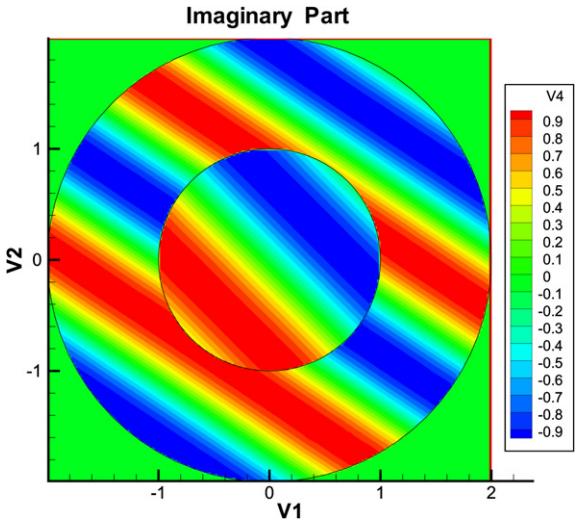

Fig. 18. Imaginary part with third order basis for 2D case.

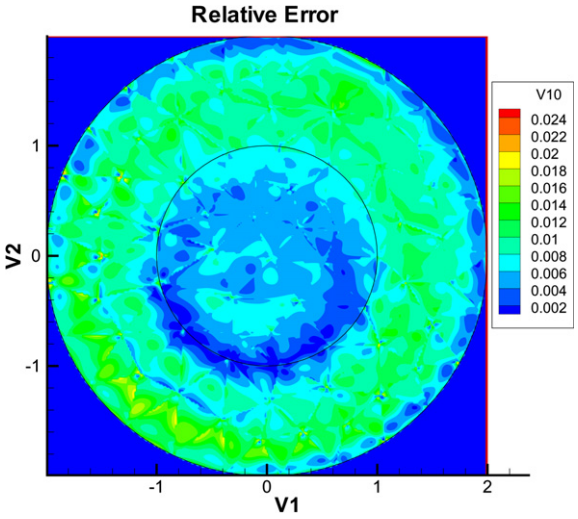

Fig. 19. Error plot with third order basis for 2D case.

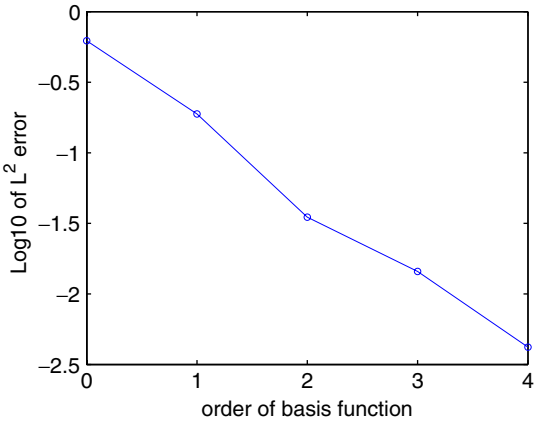

Fig. 20. Exponential decay of the L^2 error at $t = 1$ with increasing order of basis for 2D case.

6. Conclusion

In this paper, we proposed a new type of *generalized* discontinuous Galerkin (GDG) method based on distributional formulations of Schrödinger equations with nonsmooth solutions. The unique feature of the GDG method is its ability to handle general time dependent and nonlinear jump conditions. Numerical results of the GDG method have demonstrated its flexibility and high order accuracy. Meanwhile, the proposed GDG methodology can be extended to other type of partial differential equations with discontinuous solutions, which will be addressed in future work.

Acknowledgments

The authors thank the support of the National Science Foundation (Grant Nos. DMS-0408309, CCF-0513179), the Department of Energy (Grant No. DEFG0205ER25678), the NERSC Computing Award and DOD JTO MRI Contract W911NF-05-1-0517 for the work reported in this paper.

Appendix 1. Split distribution and its integration by parts formula

A.1. 1D case

We will define an evenly split $\delta(x)$ so for any function v defined in R, and $a > 0$, we have

$$\int_{-a}^{0^-} v(x)\delta(x)\mathrm{d}x = \frac{1}{2}v(0), \tag{A.1}$$

$$\int_{0^+}^{a} v(x)\delta(x)\mathrm{d}x = \frac{1}{2}v(0). \tag{A.2}$$

To justify the above, let us first define a series of functions

$$h_\epsilon(x) = \begin{cases} \frac{1}{\varepsilon}, & -\alpha\epsilon < x < \beta\epsilon \\ 0, & \text{else} \end{cases}, \tag{A.3}$$

where $0 \leqslant \alpha, \beta \leqslant 1, \alpha + \beta = 1$. In the following, we take $\alpha = \beta = \frac{1}{2}$ for an evenly-split $\delta(x)$-function. As we know,

$$\lim_{\epsilon\to 0} h_\epsilon(x) = \delta(x), \tag{A.4}$$

we define the evenly split $\delta(x)$ by the following limiting procedure,

$$\int_{-a}^{0^-} v(x)\delta(x)\mathrm{d}x \equiv \lim_{\epsilon\to 0}\int_{-a}^{0^-} v(x)h_\epsilon(x)\mathrm{d}x = \lim_{\epsilon\to 0}\frac{1}{\epsilon}\int_{-\frac{\epsilon}{2}}^{0^-} v(x)\mathrm{d}x = \lim_{\epsilon\to 0}\frac{1}{\epsilon}\left(v(x^*)\frac{\epsilon}{2}\right) = \frac{1}{2}v(0),\ x^* \in \left[-\frac{\epsilon}{2}, 0\right]$$

which is (A.1). Similarly, one can show that (A.2) can be defined.

For any piecewise continuous function $\varphi(x)$ with a jump at $x = 0$, we intend to find the integration by parts formula for a similarly defined split distribution $\frac{\partial\varphi}{\partial x}$, in the manner of (A.1) and (A.2).

Let $\varphi(x)$ have the following decomposition

$$\varphi(x) = \{\varphi\} + [\varphi]H(x) + \varphi_1(x), \tag{A.5}$$

where $\{\varphi\} = \frac{1}{2}(\varphi(0^+) + \varphi(0^-))$, $[\varphi] = \varphi(0^+) - \varphi(0^-)$, $\varphi_1(x)$ is assumed to be continuous and $\varphi_1(0) = 0$, $H(x)$ is the Heavside function

$$H(x) = \begin{cases} \frac{1}{2}, & x > 0 \\ -\frac{1}{2}, & x < 0 \end{cases}. \tag{A.6}$$

Define $H_\varepsilon(x)$ as an approximation to $H(x)$,

$$H_\varepsilon(x) = \begin{cases} \frac{1}{2}, & x > \frac{\varepsilon}{2} \\ \frac{x}{\varepsilon}, & -\frac{\varepsilon}{2} \leqslant x \leqslant \frac{\varepsilon}{2} \\ -\frac{1}{2}, & x < -\frac{\varepsilon}{2} \end{cases}, \tag{A.7}$$

and $\varphi_\epsilon(x)$ as an approximation to $\varphi(x)$,

$$\varphi_\varepsilon(x) = \{\varphi\} + [\varphi]H_\varepsilon(x) + \varphi_1(x). \tag{A.8}$$

For $v(x) \in C^\infty[a, 0], a < 0$, we define the following split distribution by a limiting procedure

$$\int_a^0 \frac{\partial\varphi}{\partial x}v(x)\mathrm{d}x \equiv \lim_{\epsilon\to 0}\int_a^0 \frac{\partial\varphi_\varepsilon}{\partial x}v(x)\mathrm{d}x.$$

To derive an integration by parts formulation for the above integral, we can decompose $v(x)$ as

$$v(x) = v_1(x) + v_2(x) \tag{A.9}$$

where $v_1(x) + v_2(x) \in C^\infty[a, 0]$, and $\mathrm{supp}(v_1) \subset [\frac{3a}{4}, 0], \mathrm{supp}(v_2) \subset [a, \frac{a}{4}]$, thus

$$v(0) = v_1(0), v(a) = v_2(a). \tag{A.10}$$

First consider

$$\begin{aligned}\int_a^0 \frac{\partial \varphi_\varepsilon}{\partial x} v_1(x)\mathrm{d}x &= [\varphi]\int_a^0 \frac{\partial H_\varepsilon}{\partial x} v_1(x)\mathrm{d}x + \int_a^0 \frac{\partial \varphi_1}{\partial x} v_1(x)\mathrm{d}x \\ &= [\varphi]\int_a^0 \frac{\partial H_\varepsilon}{\partial x} v_1(x)\mathrm{d}x + \varphi_1(0)v_1(0) - \varphi_1(a)v_1(a) - \int_a^0 \frac{\partial v_1}{\partial x}\varphi_1(x)\mathrm{d}x \\ &= [\varphi]\int_a^0 \frac{\partial H_\varepsilon}{\partial x} v_1(x)\mathrm{d}x - \int_a^0 \frac{\partial v_1}{\partial x}\varphi_1(x)\mathrm{d}x = [\varphi]\int_{-\frac{\epsilon}{2}}^0 \frac{1}{\epsilon} v_1(x)\mathrm{d}x - \int_a^0 \frac{\partial v_1}{\partial x}\varphi_1(x)\mathrm{d}x\end{aligned}$$

here $\varphi_1(0) = 0, v_1(a) = 0$ have been used in the third equality.

As $\epsilon \to 0$, using (A.10), we have

$$\begin{aligned}\int_a^0 \frac{\partial \varphi}{\partial x} v_1(x)\mathrm{d}x &= \frac{1}{2}[\varphi]v_1(0) - \int_a^0 \frac{\partial v_1}{\partial x}\varphi_1(x)\mathrm{d}x = \frac{1}{2}[\varphi]v(0) - \int_a^0 \frac{\partial v_1}{\partial x}(\varphi(x) - \{\varphi\} - [\varphi]H(x))\mathrm{d}x \\ &= \{\varphi\}v(0) - \int_a^0 \frac{\partial v_1}{\partial x}\varphi(x)\mathrm{d}x. \end{aligned} \tag{A.11}$$

Next, we consider

$$\begin{aligned}\int_a^0 \frac{\partial \varphi_\varepsilon}{\partial x} v_2(x)\mathrm{d}x &= \int_a^{\frac{a}{4}} \frac{\partial \varphi_\varepsilon}{\partial x} v_2(x)\mathrm{d}x = \int_a^{\frac{a}{4}} \frac{\partial \varphi}{\partial x} v_2(x)\mathrm{d}x = \varphi\left(\frac{a}{4}\right)v_2\left(\frac{a}{4}\right) - \varphi(a)v_2(a) - \int_a^{\frac{a}{4}} \frac{\partial v_2}{\partial x}\varphi(x)\mathrm{d}x \\ &= -\varphi(a)v(a) - \int_a^0 \frac{\partial v_2}{\partial x}\varphi(x)\mathrm{d}x,\end{aligned}$$

here $v_2(\frac{a}{4}) = 0, v_2(a) = v(a)$ have been used in the last equality.

Passing the limit $\epsilon \to 0$, we get,

$$\int_a^0 \frac{\partial \varphi}{\partial x} v_2(x)\mathrm{d}x = -\varphi(a)v(a) - \int_a^0 \frac{\partial v_2}{\partial x}\varphi(x)\mathrm{d}x. \tag{A.12}$$

Now adding (A.11) and (A.12), we have

$$\int_a^0 \frac{\partial \varphi}{\partial x} v(x)\mathrm{d}x = \{\varphi\}v(0) - \varphi(a)v(a) - \int_a^0 \frac{\partial v}{\partial x}\varphi(x)\mathrm{d}x. \tag{A.13}$$

Similarly, we can prove that, for $v(x) \in C^\infty[0, b]$,

$$\int_0^b \frac{\partial \varphi}{\partial x} v(x)\mathrm{d}x = \varphi(b)v(b) - \{\varphi\}v(0) - \int_0^b \frac{\partial v}{\partial x}\varphi(x)\mathrm{d}x. \tag{A.14}$$

Combining (A.13) and (A.14), we have

$$\int_a^b \frac{\partial \varphi}{\partial x} v(x)\mathrm{d}x = \varphi(b)v(b) - \varphi(a)v(a) - \int_a^b \frac{\partial v}{\partial x}\varphi(x)\mathrm{d}x$$

which implies for $v(x) \in C_0(-\infty, \infty)$,

$$\int_{-\infty}^{\infty} \frac{\partial \varphi}{\partial x} v(x)\mathrm{d}x = -\int_{-\infty}^{\infty} \frac{\partial v}{\partial x}\varphi(x)\mathrm{d}x,$$

defining the full Dirac $\delta(x)$ if $\varphi(x) = H(x)$.

Remark 5. In the definition of split distribution and integration by parts formula, we have selected $\alpha = \beta = \frac{1}{2}$, in principle, we could also define a general (α, β)-split distribution and its related integration by parts formula. Due to the symmetry of the Laplace operator involved in the Schrödinger equation, the evenly-split distribution is selected here.

A.2. 2D case

On the interface Γ, a local coordinate (ξ,η) will be introduced where ξ is along the normal direction of the interface and η is along the tangential direction(s). If Γ is given by the constant line $\xi=\xi^*$, we have

$$\int_K \varphi(x,y)\delta(\xi-\xi^*)\mathrm{d}x\,\mathrm{d}y=\frac{1}{2}\int_{\partial K\cap\Gamma}\frac{\varphi}{|\nabla\xi|}\,\mathrm{d}s, \tag{A.15}$$

and if $\varphi(x,y)$ is discontinuous across Γ, we have the integration by parts formula as

$$\int_K \frac{\partial\varphi}{\partial x}v(x,y)\mathrm{d}x\,\mathrm{d}y=\int_{\partial K}\widehat{\varphi}vn_x\,\mathrm{d}s-\int_K\frac{\partial v}{\partial x}\varphi(x,y)\mathrm{d}x\,\mathrm{d}y, \tag{A.16}$$

$$\int_K \frac{\partial\varphi}{\partial y}v(x,y)\mathrm{d}x\,\mathrm{d}y=\int_{\partial K}\widehat{\varphi}vn_y\,\mathrm{d}s-\int_K\frac{\partial v}{\partial y}\varphi(x,y)\mathrm{d}x\,\mathrm{d}y, \tag{A.17}$$

where

$$\widehat{\varphi}(x,y)=\begin{cases}\varphi, & \text{if } (x,y)\notin\Gamma\\ \{\varphi\}, & \text{if } (x,y)\in\Gamma\end{cases},$$

and $\{\varphi\}$ is the average of the values of φ on both sides of Γ.

To show (A.15), we first transform the triangle element K into $\widehat{K}$ in (ξ,η) coordinates as in Fig. 21, where sides of the $\widehat{K}$ are described by $\xi_1(\eta),\ \xi_2(\eta),\ \eta\in[\eta_1,\eta_2]$ and $\widehat{K}\cap\Gamma$ is given by $\xi=\xi_2(\eta)=\xi^*,\ \eta\in[\eta_1^*,\eta_2]$. Then, we have

$$\begin{aligned}\int_K\varphi(x,y)\delta(\xi-\xi^*)\mathrm{d}x\,\mathrm{d}y&=\int_{\widehat{K}}\varphi(\xi,\eta)\delta(\xi-\xi^*)\frac{\partial(x,y)}{\partial(\xi,\eta)}\,\mathrm{d}\xi\,\mathrm{d}\eta=\int_{\eta_1^*}^{\eta_2}\mathrm{d}\eta\int_{\xi_1(\eta)}^{\xi_2(\eta)}\varphi(\xi,\eta)\delta(\xi-\xi^*)\frac{\partial(x,y)}{\partial(\xi,\eta)}\,\mathrm{d}\xi\\&=\frac{1}{2}\int_{\eta_1^*}^{\eta_2}\varphi(\xi^*,\eta)\frac{\partial(x,y)}{\partial(\xi,\eta)}\Big|_{\xi=\xi^*}\mathrm{d}\eta,\end{aligned}$$

here, in second quality we can restrict our integration limit to $[\eta_1^*,\eta_2]$ instead of the full range of $[\eta_1,\eta_2]$ due to the fact that $\delta(\xi-\xi^*)=0$ for $\xi<\xi^*$. Also, the 1D split distribution formula (A.2) has been used.

Along $\Gamma=\{(x,y)=(x(\xi^*,\eta),y(\xi^*,\eta))\}$, the arc length is given by

$$\mathrm{d}s=\sqrt{x_\eta^2+y_\eta^2}\,\mathrm{d}\eta,$$

meanwhile, it is easy to check that

$$x_\eta=-\xi_x\frac{\partial(x,y)}{\partial(\xi,\eta)},\quad y_\eta=\xi_y\frac{\partial(x,y)}{\partial(\xi,\eta)},$$

then,

$$\int_K\varphi(x,y)\delta(\xi-\xi^*)\mathrm{d}x\,\mathrm{d}y=\frac{1}{2}\int_{\eta_1^*}^{\eta_2}\varphi(\xi^*,\eta)\frac{\partial(x,y)}{\partial(\xi,\eta)}|_{\xi=\xi^*}\mathrm{d}\eta=\frac{1}{2}\int_{K\cap\Gamma}\frac{\varphi}{|\nabla\xi|}\,\mathrm{d}s.$$

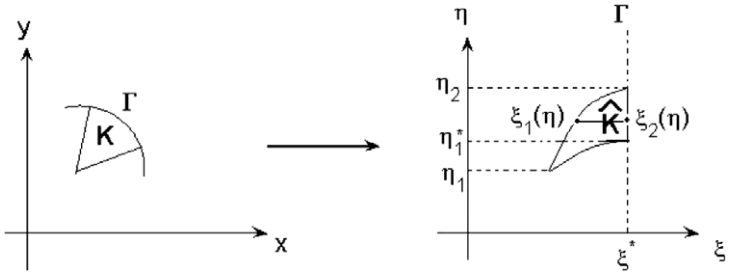

Fig. 21. Coordinate transformation on Γ.

Next, to show (A.16), we consider the three sides $\Gamma_1, \Gamma_2 = K \cap \Gamma, \Gamma_3$ of a triangle K given by $\{x_1(y), y \in [y_1, y_2]\}$, $\{x_2(y), y \in [y_1^*, y_2]\}$, $\{x_3(y), y \in [y_1, y_1^*]\}$, as depicted in Fig. 22. Then,

$$\begin{aligned}\int_K \frac{\partial \varphi}{\partial x} v \,\mathrm{d}x\,\mathrm{d}y &= \int_{y_1^*}^{y_2} \mathrm{d}y \int_{x_1(y)}^{x_2(y)} \frac{\partial \varphi}{\partial x} v \,\mathrm{d}x + \int_{y_1}^{y_1^*} \mathrm{d}y \int_{x_1(y)}^{x_3(y)} \frac{\partial \varphi}{\partial x} v \,\mathrm{d}x \\ &= \int_{y_1^*}^{y_2} \mathrm{d}y \{\varphi\} v|_{x=x_2(y)} + \int_{y_1}^{y_1^*} \mathrm{d}y \varphi v|_{x=x_3(y)} - \int_{y_1}^{y_2} \mathrm{d}y \varphi v|_{x=x_1(y)} - \int_{y_1^*}^{y_2} \mathrm{d}y \int_{x_1(y)}^{x_2(y)} \frac{\partial v}{\partial x} \varphi \mathrm{d}x \\ &\quad - \int_{y_1}^{y_1^*} \mathrm{d}y \int_{x_1(y)}^{x_3(y)} \frac{\partial v}{\partial x} \varphi \mathrm{d}x = I_1 + I_2 + I_3 - \int_K \frac{\partial v}{\partial x} \varphi \mathrm{d}x\,\mathrm{d}y,\end{aligned}$$

here the 1D integration by parts formula (A.14) is used in the second equality.

On the side $\Gamma_2 = K \cap \Gamma$ of triangle K, the arc-length is given by

$$\mathrm{d}s = \sqrt{1 + \left(\frac{\mathrm{d}x_2}{\mathrm{d}y}\right)^2}\,\mathrm{d}y,$$

and its normal direction is given by

$$(n_x, n_y) = \frac{1}{\sqrt{1 + \left(\frac{\mathrm{d}x_2}{\mathrm{d}y}\right)^2}} \left(1, -\frac{\mathrm{d}x_2}{\mathrm{d}y}\right),$$

therefore,

$$I_1 = \int_{y_1^*}^{y_2} \{\varphi\} v|_{x=x_2(y)} \,\mathrm{d}y = \int_{\Gamma_2} \{\varphi\} v \frac{1}{\sqrt{1 + (\frac{\mathrm{d}x_2}{dy})^2}} \,\mathrm{d}s = \int_{\Gamma_2} \{\varphi\} v n_x \,\mathrm{d}s.$$

Similarly, we can show that

$$I_2 = \int_{\Gamma_3} \varphi v n_x \,\mathrm{d}s, \quad I_3 = \int_{\Gamma_1} \varphi v n_x \,\mathrm{d}s,$$

therefore we have

$$I_1 + I_2 + I_3 = \int_{\partial K} \widehat{\varphi} v n_x \,\mathrm{d}s,$$

which proves (A.16). (A.17) can be similarly proven.

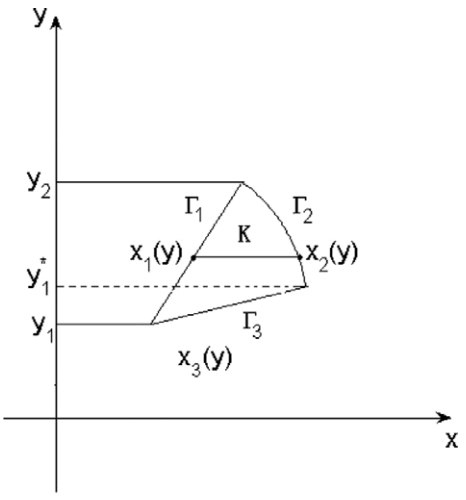

Fig. 22. Element K.

Appendix 2. Justification of δ-terms of (60a)–(60c)

We expand the function $\varphi(x,y,t)$ as

$$\varphi(x,y,t) \approx H(\xi-\xi^*)f(x,y,t) + H_1(\xi-\xi^*)g(x,y,t), \tag{A.18}$$

where $H(\xi-\xi^*)$ is the 1D Heavside function in (A.6), whose derivative along ξ-direction is $\delta(\xi-\xi^*)$, and $H_1(\xi-\xi^*)$ is a function whose derivative along ξ-direction is $H(\xi-\xi^*)$. Functions $f(x,y,t), g(x,y,t)$ will be extended away to a small neighborhood from the interface Γ by constant extension along the normal direction. It is noted that the remainder of the expansion in (A.18) will be a continuous function across Γ with continuous normal derivative.

Then, we have

$$\begin{aligned}\frac{\partial\varphi}{\partial x} &= \frac{\partial H(\xi-\xi^*)}{\partial x}f + H(\xi-\xi^*)\frac{\partial f}{\partial x} + \frac{\partial H_1(\xi-\xi^*)}{\partial x}g + H_1(\xi-\xi^*)\frac{\partial g}{\partial x}\\ &= \delta(\xi-\xi^*)\frac{\partial\xi}{\partial x}f + H(\xi-\xi^*)L_x^\xi(f,g) + H_1(\xi-\xi^*)\frac{\partial g}{\partial x},\end{aligned} \tag{A.19}$$

where $L_x^\xi(f,g)$ is defined as

$$L_x^\xi(f,g) = \frac{\partial f}{\partial x} + \frac{\partial\xi}{\partial x}g, \tag{A.20}$$

and we have

$$\frac{\partial^2\varphi}{\partial x^2} = \frac{\partial}{\partial x}\left(\delta(\xi-\xi^*)\frac{\partial\xi}{\partial x}f\right) + \delta(\xi-\xi^*)\frac{\partial\xi}{\partial x}L_x^\xi(f,g) + H(\xi-\xi^*)L_x^\xi\left(L_x^\xi(f,g),\frac{\partial g}{\partial x}\right) + H_1(\xi-\xi^*)\frac{\partial^2 g}{\partial x^2}. \tag{A.21}$$

Similarly by defining

$$L_y^\xi(f,g) = \frac{\partial f}{\partial y} + \frac{\partial\xi}{\partial y}g, \tag{A.22}$$

we have

$$\frac{\partial\varphi}{\partial y} = \delta(\xi-\xi^*)\frac{\partial\xi}{\partial y}f + H(\xi-\xi^*)L_y^\xi(f,g) + H_1(\xi-\xi^*)\frac{\partial g}{\partial y}, \tag{A.23}$$

$$\frac{\partial^2\varphi}{\partial y^2} = \frac{\partial}{\partial y}\left(\delta(\xi-\xi^*)\frac{\partial\xi}{\partial y}f\right) + \delta(\xi-\xi^*)\frac{\partial\xi}{\partial y}L_y^\xi(f,g) + H(\xi-\xi^*)L_y^\xi\left(L_y^\xi(f,g),\frac{\partial g}{\partial y}\right) + H_1(\xi-\xi^*)\frac{\partial^2 g}{\partial y^2}. \tag{A.24}$$

Notice that those terms containing $\delta(\xi-\xi^*)$ are singularities resulting from the jump conditions. Therefore, to write a PDE which is valid also at interface Γ, we must include appropriate δ-functions to compensate for the jumps as follows.

First, by introducing p and q as in (60b) and (60c), (A.19) and (A.23) becomes

$$p = H(\xi-\xi^*)L_x^\xi(f,g) + H_1(\xi-\xi^*)\frac{\partial g}{\partial x}, \tag{A.25}$$

$$q = H(\xi-\xi^*)L_y^\xi(f,g) + H_1(\xi-\xi^*)\frac{\partial g}{\partial y}, \tag{A.26}$$

where no singularity remains. Now, since

$$\frac{\partial\xi}{\partial x}L_x^\xi(f,g) + \frac{\partial\xi}{\partial y}L_y^\xi(f,g) = \left(\frac{\partial f}{\partial x}\frac{\partial\xi}{\partial x} + \frac{\partial f}{\partial y}\frac{\partial\xi}{\partial y}\right) + g\left(\left(\frac{\partial\xi}{\partial x}\right)^2 + \left(\frac{\partial\xi}{\partial y}\right)^2\right) = |\nabla\xi|\frac{\partial f}{\partial n} + |\nabla\xi|^2 g,$$

and, as we take constant extension of f along normal direction $\vec{n} = \frac{1}{|\nabla\xi|}(\frac{\partial\xi}{\partial x}, \frac{\partial\xi}{\partial y})$, i.e. $\frac{\partial f}{\partial n} = 0$, from (A.21) and (A.24), we have

$$\begin{aligned}
&\frac{\partial p}{\partial x} + \frac{\partial q}{\partial y} - \delta(\xi - \xi^*)\left(\frac{\partial \xi}{\partial x} L_x^{\xi}(f,g) + \frac{\partial \xi}{\partial y} L_y^{\xi}(f,g)\right) \\
&\quad = \frac{\partial p}{\partial x} + \frac{\partial q}{\partial y} - \delta(\xi - \xi^*)|\nabla\xi|^2 g = H(\xi - \xi^*)\left(L_x^{\xi}\left(L_x^{\xi}(f,g), \frac{\partial g}{\partial x}\right)\right. \\
&\qquad \left. + L_y^{\xi}\left(L_y^{\xi}(f,g), \frac{\partial g}{\partial y}\right)\right) + H_1\left(\frac{\partial^2 g}{\partial x^2} + \frac{\partial^2 g}{\partial y^2}\right),
\end{aligned} \tag{A.27}$$

i.e. (60a) also has no singularity left.

References

[1] M.D. Feit, J.A. Fleck Jr., Light propagation in graded-index optical fibers, Appl. Opt. 17 (24) (1978) 3990–3998.
[2] M.D. Feit, J.A. Fleck Jr., Computation of mode properties in optical fiber waveguides by a propagating beam method, Appl. Opt. 19 (7) (1980) 1154–1163.
[3] B. Cockburn, S. Hou, C.W. Shu, Tvb Runge–Kutta local projection discontinuous Galerkin finite element method for conservation laws IV: The multidimensional case, Math. Comput. 54 (1990) 545.
[4] A.H. Mohammadia, V. Shankar, W.F. Hall, Computation of electromagnetic scattering and radiation using a time domain finite volume discretization procedure, Comput. Phys. Commun. 68 (1991) 175.
[5] T. Lu, P.W. Zhang, W. Cai, Discontinuous Galerkin methods for dispersive and lossy Maxwell's equations and PML boundary conditions, J. Comput. Phys. 200 (2004) 549–580.
[6] D. Arnold, F. Brezzi, B. Cockburn, L.D. Marini, Unified analysis of discontinuous Galerkin methods for elliptic problems, SIAM J. Numer. Anal. 39 (5) (2002) 1749–1779.
[7] B. Cockburn, C.-W. Shu, The local discontinuous Galerkin method for time-dependent convection–diffusion systems, SIAM J. Numer. Anal. 35 (1998) 2440–2463.
[8] Yan Xu, Chi-Wang Shu, Local discontinuous Galerkin methods for nonlinear Schrodinger equations, J. Comput. Phys. 205 (2005) 72–97.
[9] G.A. Baker, Finite element methods for elliptic equations using nonconforming elements, Math. Comput. 31 (1977) 45–59.
[10] M.F. Wheeler, An elliptic collocation finite element method with interior penalties, SIAM J. Numer. Anal. 15 (1978) 152–161.
[11] D.N. Arnold, An interior penalty finite element method with discontinuous elements, SIAM J. Numer. Anal. 19 (1982) 742–760.
[12] D. Funaro, D. Gottlieb, A new method of imposing boundary conditions for hyperbolic equations, Math. Comput. 51 (184) (1988) 599–613.
[13] J.S. Hesthaven, D. Gottlieb, A stable penalty method for the compressible Navier–Stokes equations. I. Open boundary conditions, SIAM J. Sci. Comput. 17 (3) (1996) 579–612.